

Application of a thin intermediate cathode layer prepared by inkjet printing for SOFCs

Naoki Yashiro, Tomohiro Usui, Koichi Kikuta*

Department of Crystalline Materials Science, Graduate School of Engineering, Nagoya University, Furo-cho, Chikusa, Nagoya 464-8603, Japan

Received 8 January 2010; received in revised form 6 March 2010; accepted 2 April 2010

Abstract

The application of an inkjet printing process for fabricating solid oxide fuel cell (SOFC) cathodes was investigated. Stably-dispersed LSCF–GDC inks were prepared by ball milling, and the composition was easily controlled by the preparation process. Fabrication of an LSCF–GDC layer was successfully carried out by depositing dots and the thickness was easily controlled by repeating printing process. A planar SOFC single cell with a double-layered cathode (comprised of a paste painted cathode layer and an inkjet printed interlayer) achieved a maximum power density of 0.71 W/cm² at 600 °C. This is the preliminary work for fabricating the cathode layer of a SOFC single cell via inkjet printing.

© 2010 Elsevier Ltd. All rights reserved.

Keywords: B. Microstructure-final; C. Electrical properties; D. CeO₂; E. Fuel cells; Inkjet printing

1. Introduction

Inkjet printing technology has been widely used for fabricating 2 or 3 dimensional patterns.^{1–4} This patterning process works by moving print heads precisely to the desired positions on the substrate and depositing inks as required. This on-demand process has many advantages. First, positioning accuracy is high, which enables fine pattern formation. Second, patterns are fabricated by arranging dots tens to several hundred of microns in diameter, enabling fabrication of various patterns sizes. Third, this process can be performed without contacting substrates, which enables printing on both planar and curved substrates. Finally, the production reproducibility is high, which enables mass-production of fine patterns of consistent quality. We utilized these advantages in our application of the inkjet printing to the fabrication of SOFC single cells.

A solid oxide fuel cell (SOFC) is an electrochemical reactor with utilizing a ceramic ion conductor electrolyte.^{5,6} Because SOFCs operate at elevated temperatures (400–1000 °C), electric power can be generated efficiently and no need for an expensive noble metal catalyst. Consequently, SOFCs are expected to

be used in a variety fields such as co-generation systems, various power sources, exhaust gas purification, and hydrogen-gas manufacturing.

For the practical application of SOFCs, however, further improvements in volumetric power, system reliability and power unit production efficiency are required. Among these items, improvement of the volumetric power is especially important for smaller systems such as portable power sources (e.g. auxiliary power units). For that purpose, there are two possible approaches: (1) improvement of single cell output power and (2) the accumulation of many single cells for fabricating SOFC stacks.^{7–9} Both of these approaches are capable of broadening the application field of SOFC systems.

In order to improve the output power of a single cell, the thickness and microstructure of the electrolyte and electrode layers must be optimized. A dense, thin electrolyte layer can separate oxidation gas from fuel gas. In contrast, a porous cathode and anode composed of a mixture of electrode and electrolyte materials are preferable for decreasing polarization. Such porous electrodes can lead to the expansion of triple phase boundaries (TPBs) at the interface of electrode, electrolyte, and gas phases, which promotes electrode reaction.^{10,11} Moreover, both the electrolyte and the electrodes must be of appropriate thickness, leading to lower electric and diffusion resistance for oxidation and fuel gases.

* Corresponding author. Tel.: +81 52 789 3345; fax: +81 52 789 3182.
E-mail address: kik@apchem.nagoya-u.ac.jp (K. Kikuta).

In the present work, improvement in output power and production efficiency of cells was investigated using inkjet printing. So far, the application of inkjet printing to the fabrication of various ceramic components has been studied by many researchers.^{12–16} However, only a few articles have been reported regarding the fabrication of SOFCs by the inkjet printing.^{17,18} Furthermore, no research on the fabrication of cathode layers by inkjet printing with aqueous inks has been reported.

In this study, we first conducted fundamental research on the preparation of aqueous slurry inks, along with printing and heating conditions. Next, the performance of the fabricated cells with different cathode layers was evaluated by electrochemical analysis.

2. Experimental

2.1. Preparation of aqueous inks

Ceramic inks were prepared from commercially available powders; $\text{La}_{0.6}\text{Sr}_{0.4}\text{Co}_{0.2}\text{Fe}_{0.8}\text{O}_{3-\delta}$ (LSCF; LSCF-6428F, Average grain size $\sim 2.44\ \mu\text{m}$, Daiichi Kigenso Kagaku Kogyo Co., Ltd.) and $\text{Ce}_{0.9}\text{Gd}_{0.1}\text{O}_{1.95}$ (GDC; CGO 90/10 SY ULSA, Average grain size $\sim 0.44\ \mu\text{m}$, Anan Kasei Co., Ltd.). At the beginning, evaluation of the dispersion stability of LSCF and GDC powders was carried out by monitoring the ζ -potential (ELSZ-1, Otsuka Electronics Co., Ltd.). Based on these results, a preparation process of LSCF–GDC inks was proposed as shown in Fig. 1. A polymer dispersant (carboxylic acid ammonium salt copolymer, A-6114, Toa Gosei Co., Ltd.), LSCF, and GDC were added into the ammonia water with pH 10, followed by ball milling for 48 h using YSZ ball (3 mm in diameter). Preparation of an ink with the ratio of LSCF/GDC = 60/40 was carried out, since several articles have reported that cathode powder with an LSCF/GDC composition in the range of 50/50 to 60/40 is appropriate for this system.^{19–21} Moreover, viscosity and powder concentration of the prepared ink should be 1–2 mPa s and over 3 mass%, respectively, for efficient printing of the cathode layer using this process. The LSCF/GDC composition in each ink was confirmed by energy dispersive X-ray spectroscopy (EDX; EX-54140 MSK, JEOL). The viscosity of each ink was measured by rotary viscometer (E-type Visconic, Tokyo Keiki Inc.), and the powder concentration of each ink was also calculated from the weight loss by the heating using TG-DTA (Thermo Plus TG 8101D, Rigaku Corp.). In addition, the particle size distribution of LSCF, GDC, and the prepared inks was

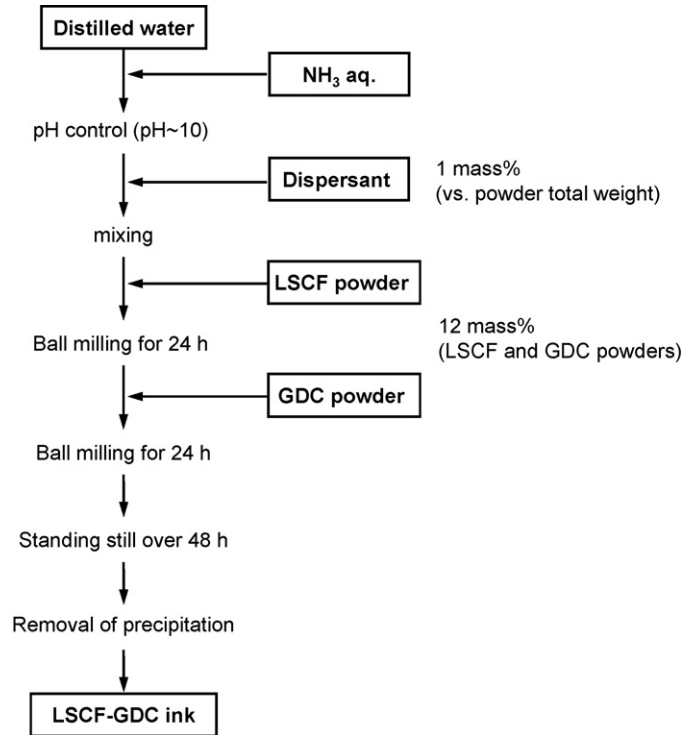


Fig. 1. Preparation of LSCF–GDC inks.

measured using a particle size distribution analyzer (LA-920, HORIBA, Ltd.).

2.2. Fabrication of LSCF–GDC layers by inkjet printing

We prepared electrolyte–anode double layer stack print substrates by laminating an electrolyte green sheet on an anode green sheet. The fabrication procedure of each green sheet is described in our previous paper.²² The thickness of the electrolyte and anode layers after heat treatment was around 50 and 600 μm , respectively.

An LSCF–GDC cathode layer was fabricated by a commercial single-nozzle printer (Pico Jet-1000, MICROJET Co., Ltd.) on the double-layered substrate, then, followed by the heat treatment. This printer has a nozzle with an internal diameter of 50 μm and the volume of a discharged droplet is around 50 pL. Another conventional painting process was also used with and without the inkjet printing in the same manner as previous reports. After deposition of the cathode layer, heat treatment of these cells was carried out at 1000 °C for 2 h. The surface

Table 1
Fabricated planar cells.

	Cell 1	Cell 2	Cell 3
Cathode	LSCF–GDC (I. J. printed)	LSCF–GDC (painted)	LSCF–GDC (painted)LSCF–GDC (I. J. printed)
Electrolyte	GDC	GDC	GDC
Anode	NiO–GDC	NiO–GDC	NiO–GDC
Schematic			

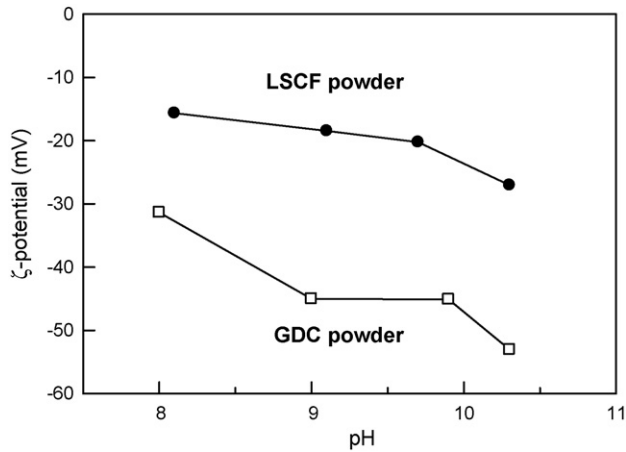


Fig. 2. ζ -potential of LSCF and GDC powders as a function of pH.

profiles of deposited dots were measured with an optical microscope (BX60, Olympus Corp.), and the microstructures of the prepared cells were imaged with a scanning electron microscope (SEM; JSM 5600, JEOL).

2.3. Evaluation of cell electrochemical performance of the cell

In this study, three types of cells with different cathodes were fabricated by inkjet printing and/or conventional a painting process using LSCF–GDC (60/40) as shown in Table 1. The cathode layers in Cells 1–3 are as follows:



Fig. 3. LSCF–GDC ink after sedimentation test lasting 1 month.

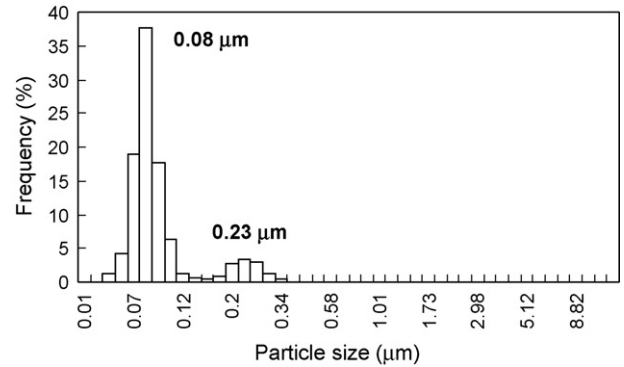


Fig. 4. Particle size distribution of prepared LSCF–GDC ink.

Cell 1: single layer cathode with a thickness of $\sim 3 \mu\text{m}$ fabricated via inkjet printing.

Cell 2: single layer cathode with a thickness of $30 \mu\text{m}$ fabricated via painting.

Cell 3: combined double-layered cathode; painted layer on inkjet printed layer with a total thickness of $32 \mu\text{m}$.

A silver paste (TR-6182, Tanaka Precious Metal) was also painted on both electrodes of the specimens as a current collector and dried at 100°C . Fuel cell performance was measured using a frequency response analyzer (FRA; Solartron 1255B) and a potentiogalvanostat (Solartron SI1287) system. A hydrogen/nitrogen gas mixture humidified with water at 30°C and air were used as the fuel and oxidant gases, respectively, with a flow rate of 40 mL/min .

3. Results and discussion

3.1. Evaluation of prepared inks

3.1.1. Dispersion stability of LSCF and GDC powders

First, dispersion stability of LSCF and GDC powders was evaluated separately. The results of ζ -potential measurements under weak alkaline conditions are shown in Fig. 2, indicating that the GDC powder has larger ζ -potential than LSCF powder and the absolute values of both potentials increase with pH. As a result, strong repulsion among these particles can be expected over pH 10. Dispersion stability of each powder was evaluated after milling by placing it into alkaline water (pH 10) for 48 h. The LSCF slurry remained in a stable dispersion state for more than 1 month, whereas the GDC powder showed signs of sedimentation within 2 days.

The differences in dispersion behavior of the LSCF and GDC powders seemed to arise from differences in density and particle size. Although GDC particles have a large ζ -potential, they agglomerate easily by bridging, and sediment begins to occur due to the increase in density. In contrast, LSCF can be deflocculated at pH 10 because the dispersant is easily adsorbed on the surface of particles by the van der Waals attraction. Furthermore, the carboxylic group of the dispersant molecule ionizes at pH 10, which stabilize the dispersion state of LSCF by the both steric and electrostatic repulsion forces. Based on these results,

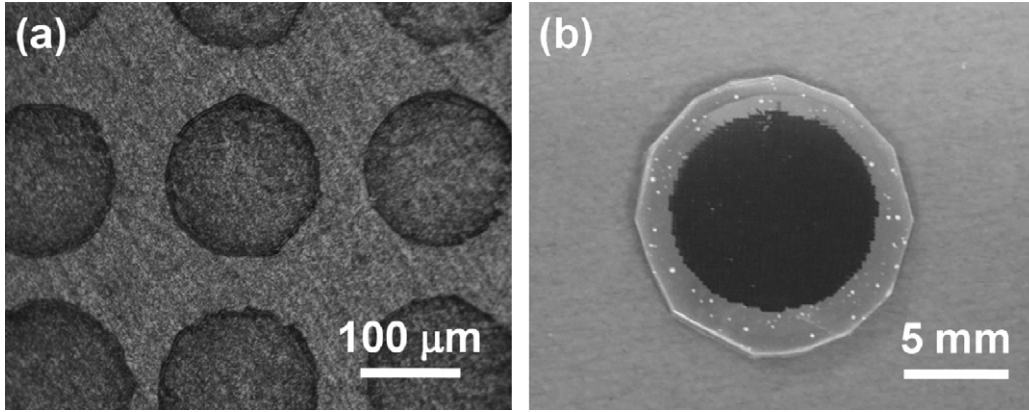


Fig. 5. LSCF-GDC pattern fabricated by inkjet printing: (a) microscopic image of deposited dots and (b) appearance of fabricated LSCF-GDC layer on a laminated substrate.

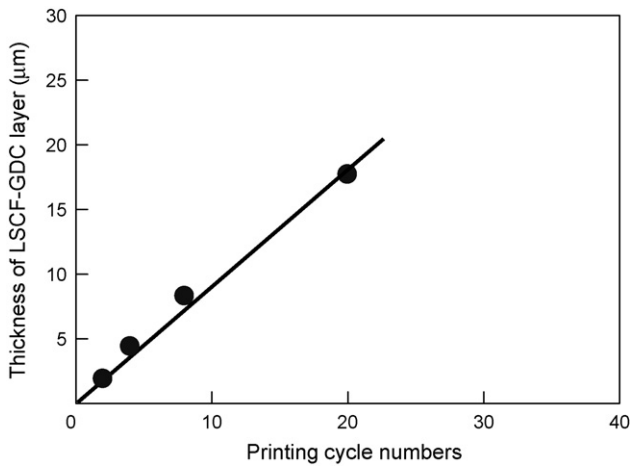


Fig. 6. Thickness of LSCF-GDC cathode layer with respect to cycle numbers of printing.

we tried to improve the dispersion state by the interaction of dispersed LSCF with GDC particles through the experimental procedure as described in Fig. 1. LSCF powder is first treated by ball milling, then GDC powder was added to this LSCF suspension and additional ball milling was carried out. The dispersants

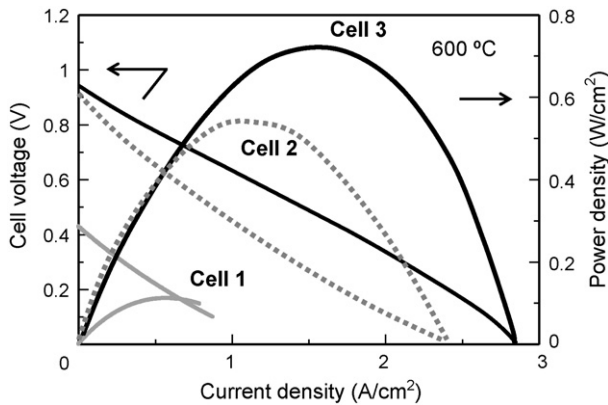


Fig. 7. Fuel cell performance of Cells 1, 2, and 3 operated at 600 °C. Cell voltage and power density as a function of current density. Cathode gas (oxidant): air, 40 mL/min. Anode gas (fuel): N₂, 10 mL/min + H₂, 30 mL/min.

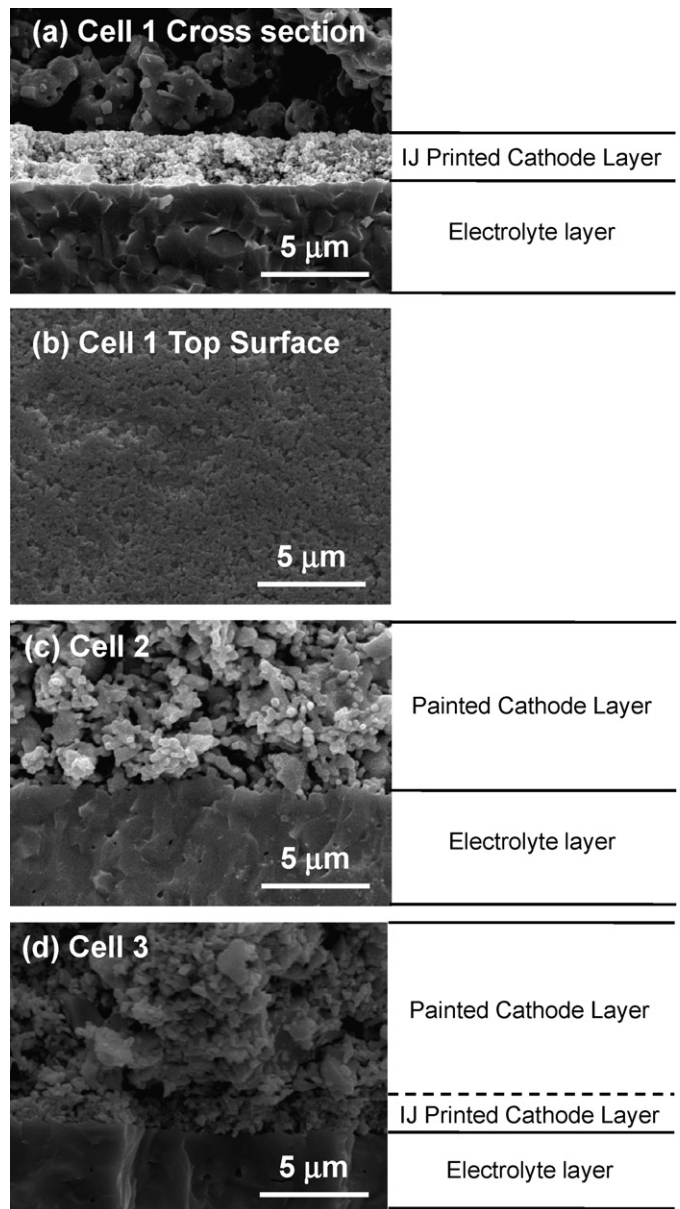


Fig. 8. SEM images of LSCF-GDC layers. (a) Cross-section of Cell 1, (b) dense top surface of Cell 1, (c) cross-section of Cell 2, and (d) cross-section of Cell 3.

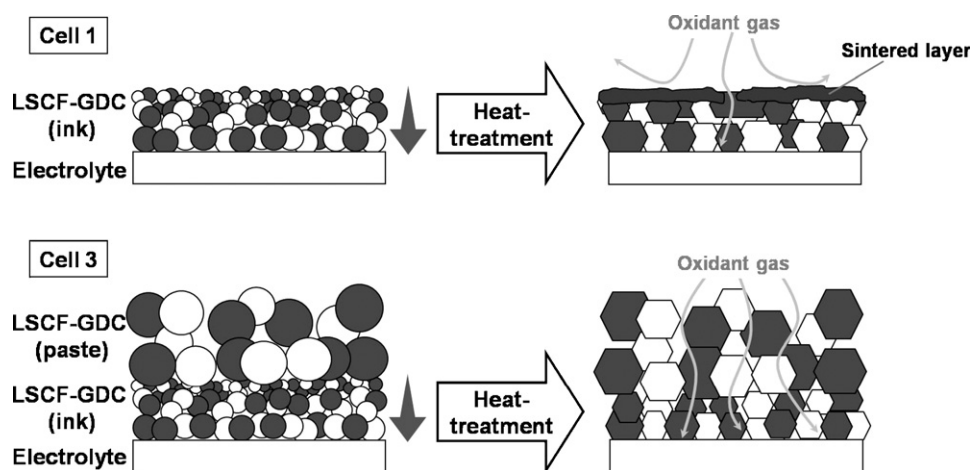


Fig. 9. Microstructure development of LSCF–GDC cathode layers in Cell 1 and Cell 3.

adsorbed on LSCF particles seemed to interact strongly with GDC particles, preventing agglomeration and sedimentation of GDC particles in the mixture slurry.

3.1.2. Evaluation of LSCF–GDC inks

The mixture slurry shown in Fig. 3 remained stable for more than 1 month and can be used as an ink for the following inkjet printing process. An ink prepared from a 60/40 mixture of LSCF/GDC powders gave a final composition of LSCF/GDC = 57/43. It was also confirmed that other inks prepared with starting compositions of LSCF/GDC ranging from 40/60 to 80/20 also retained their starting compositions within 3 mass%. These results suggest that the composition of the ink can be easily adjusted through modifications in the starting powder composition. Total powder content in each ink was confirmed by heat treatment up to 600 °C, demonstrating that the prepared slurry with LSCF/GDC = 57/43 includes almost 5 mass% mixture powder. The viscosity of prepared ink was confirmed to be around 1 mPa s, which is low enough to use for inkjet printing with the equipment used in this experiment. It is noteworthy that the particle size distribution in Fig. 4 reveals that the particles are much finer than the starting powders and have a bimodal distribution, suggesting that both LSCF and GDC were milled into very fine powder, which improves the dispersion stability of inks.

3.2. Evaluation of LSCF–GDC layer fabricated by inkjet printing

The ink with the composition of LSCF/GDC = 57/43 was used in this study, as previously described in Section 2.1. The LSCF–GDC cathode layer was inkjet printed on electrolyte-anode stacks. Fig. 5(a) shows the deposited dots (150 μm in diameter) on the substrate. Here, the coffee ring phenomena is clearly visible (i.e. that particles in the deposited drop move towards the edge of the dot during drying^{23,24}), which might effect on the following surface densification of the deposited cathode layer. By depositing these dots closely, a desired pattern or film layer was successfully fabricated as shown in Fig. 5(b).

So far, the minimum thickness of the deposited film was 2 μm, and was increased linearly with increasing printing cycle numbers as shown in Fig. 6, which indicates the controllability of the thickness of the cathode layer and good reproducibility of this printing process.

3.3. Electrochemical performance of the fabricated cells

Fuel cell performance of the Cells indicated in Table 1 was shown in Fig. 7. The open circuit voltages (OCVs) of Cells 1, 2, and 3 were 0.43, 0.92 and 0.94 V, respectively, and the maximum power densities were 0.11, 0.54 and 0.71 W/cm², respectively. Cell 1 printed by the inkjet process showed a smaller OCV and maximum power density compared with Cell 2 prepared by the conventional printing method. On the other hand, Cell 3 with a double-layered cathode showed a larger OCV and a higher maximum density of 0.71 W/cm², which is rather good performance in this LSCF–GDC/GDC/NiO–GDC system.^{19,25,26}

These results seem to be related to the microstructure development of cathode layers during the heating stage, since these three cells here have the same anode and electrolyte sheets. Fig. 8(a), (c) and (d) show the cross-sectional SEM micrographs of the prepared cells. Important factors influencing the electric performance could be the amount of TPBs and oxidant gas permeability into cathode layer. TPBs are known to be present at the interface of cathode particles, electrolyte particles, and the oxidant gas phase, which will be increased using finer powders. As characterized in the previous section, the prepared cathode ink is composed of very fine particles (less than 0.4 μm in diameter) which is desirable to create a larger area for reaction to occur but could be easily sintered at elevated temperatures compared with the cathode paste used to make the cathode layer of Cell 2. In fact, a dense sintered layer can be observed at the top surface of the cathode layer in Cell 1 as in Fig. 8(a) and (b), which suppresses the gas permeation closely related to the poor electric performance. Although such a dense surface layer cannot be observed in Cell 2, the performance of the Cell 2 is not superior to that of Cell 3 because of smaller amount of TPBs.

Cell 3 has a unique graded microstructure without forming the dense surface layer that was observed in the Cell 1. This is because the top surface of the inkjet printed layer is covered with a painted layer with larger grains (approximately a few microns in diameter), which sintered with the finer inkjet printed layer preferably during the heating stage. Microstructure development during the sintering is schematically shown in Fig. 9. So the resultant IJ printed cathode layer in Cell 3 is slightly thinner than that in Cell 1 covered with a dense surface layer. Further detailed research on the addition of pore formers to enhance gas permeation and on the control of the intermediate cathode layer including much TPBs is also required to obtain better performance.

4. Conclusions

In the present work, inkjet printing has been successfully applied to the fabrication of SOFC cathode layers using an aqueous ink prepared by ball milling. A stably-dispersed aqueous ink with of target composition, viscosity, and powder content was obtained by optimizing the preparation process. Moreover, it was confirmed that the desired pattern was fabricated by depositing dots, and the layer thickness was easily controlled through variation in printing cycle numbers. However, the particles in the inkjet printed layer were very fine due to the milling process and the cathode layer has a graded size distribution with respect to depth due to the effect of gravity. This caused the surface of the heated cathode to form a dense surface layer, which resulted in poor gas permeation. This method is, however, very effective for improving cell performance when the inkjet printed layer is introduced between the electrolyte and a painted cathode layer composed of larger particles. The cell with the double-layered cathode showed superior performance with an OCV of 0.94 V and a maximum power density of 0.71 W/cm² at 600 °C. This is because the inkjet printed layer gave rise to a large quantity of TPBs without forming a dense surface layer.

Acknowledgements

The authors acknowledge Anan Kasei Co., Ltd. for supplying the GDC powder. This work has been supported by NEDO, Japan, as part of the Advanced Ceramic Reactor Project.

References

- Calvert P. Inkjet printing for materials and devices. *Chemistry of Materials* 2001;**13**:3299–305.
- Xue F, Liu Z, Su Y, Varahramyan K. Inkjet printed silver source/drain electrodes for low-cost polymer thin film transistors. *Microelectronic Engineering* 2006;**83**:298–302.
- Roth EA, Xu T, Das M, Gregory C, Hickman JJ, Boland T. Inkjet printing for high-throughput cell patterning. *Biomaterials* 2004;**25**:3707–15.
- Kobayashi H, Kanbe S, Seki S, Kiguchi H, Kimura M, Yudasaka I, Miyashita S, Shimoda T, Towns CR, Burroughes JH, Friend RH. A novel RGB multicolor light-emitting polymer display. *Synthetic Metals* 2000;**111–112**:125–8.
- Minh NQ. Ceramic fuel cells. *Journal of the American Ceramic Society* 1993;**76**:563–88.
- Steele BCH. Appraisal of Ce_{1-y}Gd_yO_{2-y/2} electrolytes for IT-SOFC operation at 500 °C. *Solid State Ionics* 2000;**129**:95–110.
- Suzuki T, Funahashi Y, Yamaguchi T, Fujishiro Y, Awano M. Development of cube-type SOFC stacks using anode-supported tubular cells. *Journal of Power Sources* 2008;**175**:68–74.
- Yamaguchi T, Shimizu S, Suzuki T, Fujishiro Y, Awano M. Fabrication and characterization of high performance cathode supported small-scale SOFC for intermediate temperature operation. *Electrochemistry Communications* 2008;**10**:1381–3.
- Shao Z, Haile SM. A high-performance cathode for the next generation of solid-oxide fuel cells. *Nature* 2004;**431**:170–3.
- Mogensen M, Skaarup S. Kinetic and geometric aspects of solid oxide fuel cell electrodes. *Solid State Ionics* 1996;**86–88**:1151–60.
- Williford RE, Chick LA, Maupin GD, Simmer SP, Stevenson JW. Diffusion limitations in the porous anodes of SOFCs. *Journal of the Electrochemical Society* 2003;**150**:A1067–72.
- Song JH, Edirisinghe MJ, Evans JRG. Formulation and multilayer jet printing of ceramic inks. *Journal of the American Ceramic Society* 1999;**82**:3374–80.
- Lewis JA. Direct-write assembly of ceramics from colloidal inks. *Current Opinion in Solid State and Materials Science* 2003;**6**:245–50.
- Ramakrishnan N, Rajesh PK, Ponnambalam P, Prakasan K. Studies on preparation of ceramic inks and simulation of drop formation and spread in direct ceramic inkjet printing. *Journal of Materials Processing Technology* 2005;**169**:372–81.
- Noguera R, Lejeune M, Chartier T. 3D fine scale ceramic components formed by ink-jet prototyping process. *Journal of the European Ceramic Society* 2005;**25**:2055–9.
- Blazdell PF, Evans JRG. Application of a continuous ink jet printer to solid freeforming of ceramics. *Journal of Materials Processing Technology* 2000;**99**:94–102.
- El-Toni AM, Yamaguchi T, Shimizu S, Fujishiro Y, Awano M. Development of a dense electrolyte thin film by the ink-jet printing technique for a porous LSM substrate. *Journal of the American Ceramic Society* 2008;**91**(1):346–9.
- Young D, Sukeshini AM, Cummins R, Xiao H, Rottmayer M, Reitz T. Inkjet printing of electrolyte and anode functional layer for solid oxide fuel cells. *Journal of Power Sources* 2008;**184**:191–6.
- Leng Y, Chan SH, Liu Q. Development of LSCF–GDC composite cathodes for low-temperature solid oxide fuel cells with thin film GDC electrolyte. *International Journal of Hydrogen Energy* 2008;**33**:3808–17.
- Fan B, Liu X. A-deficit LSCF for intermediate temperature solid oxide fuel cells. *Solid State Ionics* 2009;**180**:973–7.
- Qiang F, Sun KN, Zhang NQ, Zhu XD, Le SR, Zhou DR. Characterization of electrical properties of GDC doped A-site deficient LSCF based composite cathode using impedance spectroscopy. *Journal of Power Sources* 2007;**168**:338–45.
- Kubota C, Ito Y, Kikuta K. Co-firing of LSM–GDC/GDC/NiO–GDC with addition of nano-GDC powder. *Journal of the Ceramic Society of Japan* 2008;**116**(7):792–6.
- Chow E, Herrmann J, Barton CS, Raguse B, Wieczorek L. Inkjet-printed gold nanoparticle chemiresistors: influence of film morphology and ionic strength on the detection of organics dissolved in aqueous solution. *Analytica Chimica Acta* 2009;**632**:135–42.
- Wang J, Evans JRG. Drying behaviour of droplets of mixed powder suspensions. *Journal of the European Ceramic Society* 2006;**26**:3123–31.
- Zhen YD, Tok AIY, Jiang SP, Boey FYC. Fabrication and performance of gadolinia-doped ceria-based intermediate-temperature solid oxide fuel cells. *Journal of Power Sources* 2008;**178**:69–74.
- Fu C, Chan SH, Liu Q, Ge X, Pasciak G. Fabrication and evaluation of Ni-GDC composite anode prepared by aqueous-based tape casting method for low-temperature solid oxide fuel cell. *International Journal of Hydrogen Energy* 2010;**35**:301–7.